

SUPPLEMENTAL FILES

Suppression of Resting Metabolism by the Angiotensin AT₂ Receptor

Nicole K. Littlejohn¹, Henry L. Keen¹, Benjamin J. Weidemann¹, Kristin E. Claflin¹, Kevin V. Tobin¹, Kathleen R. Markan¹, Sungmi Park¹, Meghan C. Naber¹, Francoise A. Gourronc², Nicole A. Pearson¹, Xuebo Liu¹, Donald A. Morgan¹, Aloysius J. Klingelhutz^{2,3}, Matthew J. Potthoff^{1,3,4}, Kamal Rahmouni^{1,3,4,5,6}, Curt D. Sigmund^{1,3,4,5,6},
and Justin L. Grobe^{1,3,4,5,6}

Departments of ¹Pharmacology and ²Microbiology, ³Fraternal Order of Eagles' Diabetes Research Center, ⁴Obesity Research and Education Initiative, ⁵François M. Abboud Cardiovascular Research Center, and ⁶Center for Hypertension Research, University of Iowa, Iowa City, IA 52242

Running Title: Adipocyte AT₂ Suppresses Resting Metabolism

Co-Corresponding Authors:

Justin L. Grobe, PhD
Department of Pharmacology
University of Iowa
51 Newton Rd., 2-307 BSB
Iowa City, IA 52242
Tel: (319) 353-5789
Fax: (319) 335-8930
Email: justin-grobe@uiowa.edu

Curt D. Sigmund, PhD
Department of Pharmacology
University of Iowa
51 Newton Rd., 2-471B BSB
Iowa City, IA 52242
Tel: (319) 335-7946
Fax: (319) 335-8930
Email: curt-sigmund@uiowa.edu

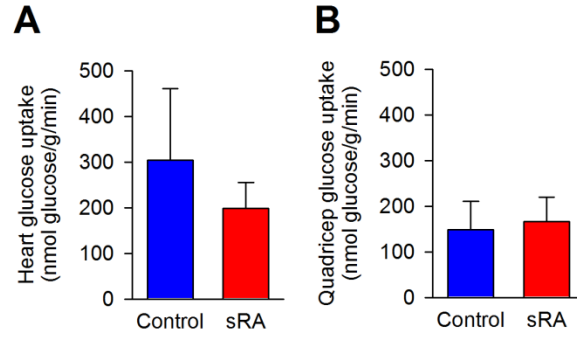


Figure S1. No change in cardiac and skeletal muscle glucose uptake – related to Figure 1. (A) Heart glucose uptake in control (N=8; 4 males and 4 females) and sRA (N=7; 3 males and 4 females) mice. (B) Quadriceps skeletal muscle glucose uptake in control (N=8; 4 males and 4 females) and sRA (N=7; 3 males and 4 females) mice. All data presented as mean \pm sem. * $p < 0.05$ was considered significant.

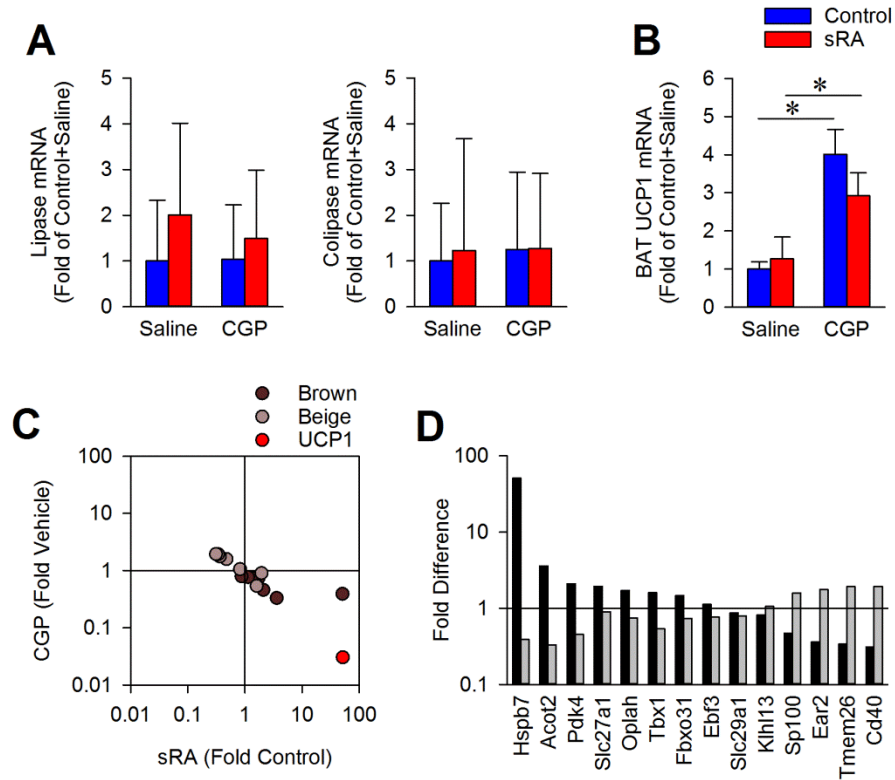


Figure S2. AT_2 activation altered beige marker in iWAT with no change in pancreatic enzyme expression or BAT UCP1 – related to Figure 2 and Table S2. (A) Lipase and colipase mRNA from the pancreas isolated from control (N=7 per group) and sRA (N=5 per group) mice treated with saline or CGP. (B) UCP1 mRNA from BAT isolated from control and sRA mice treated with saline or CGP (N=6 per group). (C-D) Beige and brown markers from the transcriptome (N=3). All data presented as mean \pm sem. * $p < 0.05$ was considered significant.

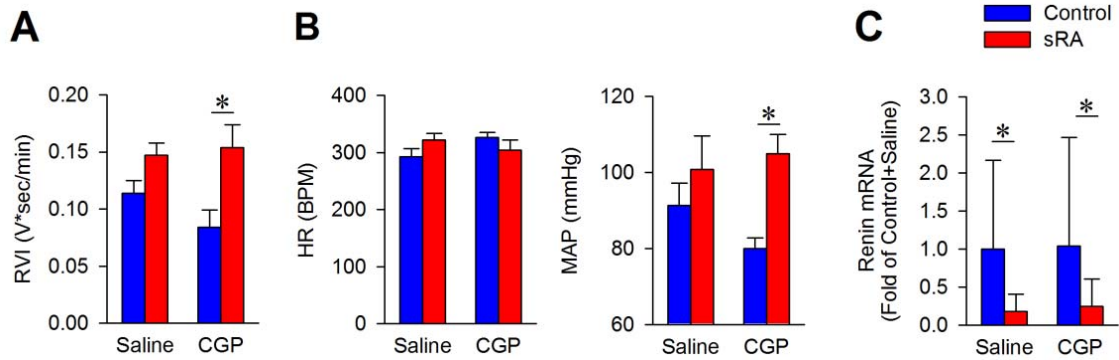


Figure S3. AT_2 activation does not reduce SNA – related to Figure 3. (A) Quantification of intact nerve electrical activity by the RVI methods. Con+sal N=10 (3 males, 7 females); sRA+sal N=10 (3 males, 7 females); Con+CGP N=8 each (2 males, 6 females); sRA+CGP N=8 each (2 males, 6 females). (B) Under anesthesia, heart rate (HR) and mean arteriole pressure (MAP) were measured during nerve recording procedures Con+Sal N=10 (3 males, 7 females); sRA+sal N=10 (3 males, 7 females); Con+CGP N=8 each (2 males, 6 females); sRA+CGP N=8 each (2 males, 6 females). (C) Renal renin mRNA levels from control and sRA mice treated with saline or CGP (N=6 per group). All data presented as mean \pm sem. * $p < 0.05$ was considered significant.

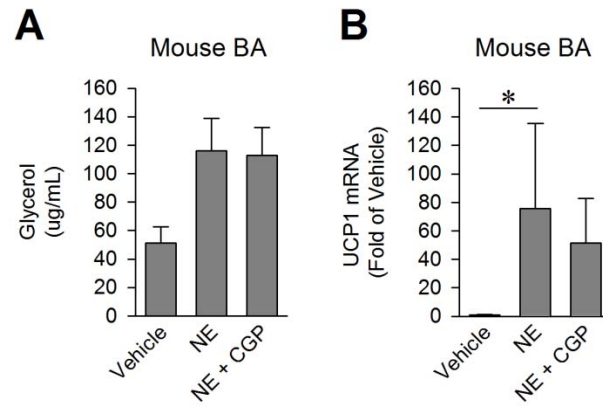


Figure S4. AT₂ activation does not alter norepinephrine induced UCP1 in brown adipocytes (BA) – related to Figure 4. (A) Glycerol in the media from mouse primary adipocytes isolated from BAT treated for 6 hours with vehicle, NE (10 μ M), or NE and CGP (10 nM) (N=6 per group). (B) UCP-1 mRNA in mouse primary adipocytes isolated from the BAT. All data presented as mean \pm sem. * $p < 0.05$ was considered significant.

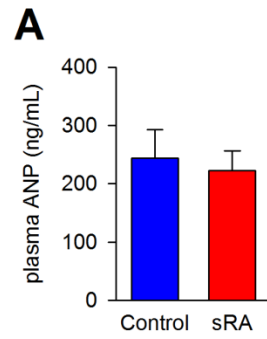


Figure S5. No difference in plasma ANP – related to Figure 5. (A) Plasma ANP levels from control and sRA mice (N=6; 3 males, 3 females). All data presented as mean \pm sem. * $p < 0.05$ was considered significant.

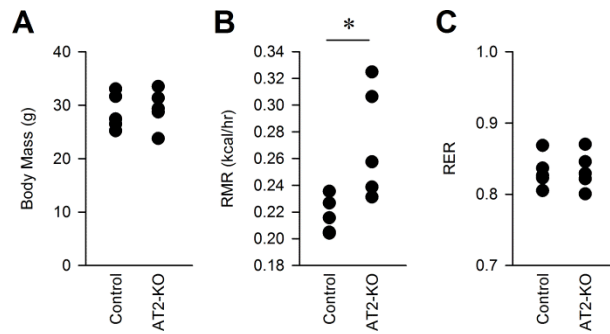


Figure S6. Increased baseline RMR in AT2-KO mice – related to Figure 6. (A) Body mass, (B) RMR assessed at thermoneutrality (30°C), and (C) RER in AT2-KO (n=5) and littermate control (n=5) male mice. * $p < 0.05$ was considered significant.

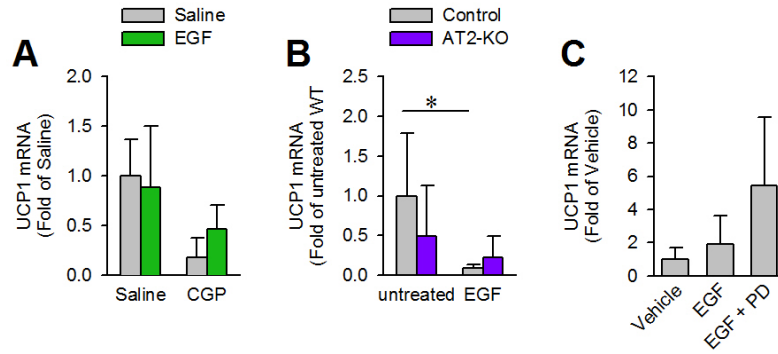


Figure S7. No increased UCP1 expression with EGF treatment – related to Figure 6. (A) UCP1 mRNA in iWAT from wild-type C57BL/6J male mice treated for 2 weeks with saline, EGF, CGP, or EGF + CGP (N=5 per group). (B) UCP1 mRNA in iWAT from control and AT₂-KO mice at baseline or after 2 week treatment with EGF (N=5 per group). (C) UCP1 mRNA from primary mouse white adipocytes treated with vehicle, EGF (100 ng/mL), or EGF and PD (10 uM) for 6 hrs (N=7 per group). All data presented as mean \pm sem. * $p < 0.05$ was considered significant.

Table S1. Body composition of sRA mice – related to Figure 1.

<i>Parameter</i>	<i>Control Male</i>	<i>sRA Male</i>	<i>Control Female</i>	<i>sRA Female</i>	<i>sRA Genotype Main Effect</i>	<i>Sex Main Effect</i>	<i>sRA Genotype X Sex Interaction</i>
Number of mice (male)	4	4	4	4			
Body mass (g)	30.7 ± 1.4	21.8 ± 1.4	25.7 ± 1.4	18.5 ± 1.4	P=0.013	P<0.001	P=0.533
Fat mass (g)	5.5 ± 0.8	2.7 ± 0.8	6.4 ± 0.8	4.1 ± 0.8	P=0.204	P=0.011	P=0.762
Lean mass (g)	20.5 ± 0.5	16.1 ± 0.5	16.5 ± 0.5	12.8 ± 0.5	P<0.001	P<0.001	P=0.510
Fluid mass (g)	4.1 ± 0.2	2.6 ± 0.2	3.3 ± 0.2	2.2 ± 0.2	P=0.015	P<0.001	P=0.444
Fat (%)	17.4 ± 2.2	12.4 ± 2.2	24.5 ± 2.2	22.4 ± 2.2	P=0.002	P=0.140	P=0.537
Lean (%)	67.5 ± 2.3	74.2 ± 2.3	64.6 ± 2.3	69.9 ± 2.3	P=0.147	P=0.024	P=0.784
Fluid (%)	13.4 ± 0.3	12.0 ± 0.3	12.9 ± 0.3	11.7 ± 0.3	P=0.141	P<0.001	P=0.631

* P<0.05 vs. Saline, and † P<0.05 vs. CGP-42122a. All data presented as mean ± se of LS mean.

Table S2. Role of AT₂ on tissue masses in sRA and control mice – related to Figure 2.

<i>Parameter</i>	<i>Control + Saline</i>	<i>sRA + Saline</i>	<i>Control + CGP</i>	<i>sRA + CGP</i>	<i>Gender Main Effect</i>	<i>Genotype Main Effect</i>	<i>Drug Main Effect</i>
Number of mice	17	9	16	8			
<i>Males</i>	10	5	10	5			
<i>Females</i>	7	4	6	3			
Age at sacrifice (weeks)	15.7 ± 0.2	15.6 ± 0.2	15.6 ± 0.2	15.7 ± 0.2	P=0.270	P=0.717	P=0.947
<i>Males</i>	15.8 ± 0.2	15.5 ± 0.2	15.5 ± 0.2	15.9 ± 0.1			
<i>Females</i>	15.3 ± 0.3	15.8 ± 0.2	15.6 ± 0.3	15.2 ± 0.4			
Body mass (g)	25.0 ± 1.8	17.8 ± 0.5 *	28.3 ± 2.3 *	23.1 ± 2.1 †	P=0.003	P=0.002	P=0.017
<i>Males</i>	27.6 ± 1.3	17.6 ± 1.3	32.4 ± 1.6	25.5 ± 2.7			
<i>Females</i>	21.1 ± 0.6	17.9 ± 0.5	22.7 ± 2.5	19.9 ± 2.5			
BAT (mg)	82 ± 20	77 ± 10	58 ± 6	54 ± 10	P=0.509	P=0.784	P=0.126
<i>Males</i>	70 ± 7	64 ± 9	61 ± 9	56 ± 15			
<i>Females</i>	98 ± 49	95 ± 18	54 ± 9	49 ± 16			
iWAT (mg)	247 ± 22	187 ± 10 *	299 ± 23	165 ± 13	P=0.867	P<0.001	P=0.399
<i>Males</i>	276 ± 24	168 ± 12	285 ± 24	165 ± 19			
<i>Females</i>	207 ± 38	211 ± 5	328 ± 53	164 ± 21			
eWAT (mg)	364 ± 42	180 ± 14 *	398 ± 38	190 ± 16	P=0.087	P<0.001	P=0.413
<i>Males</i>	461 ± 52	183 ± 17	394 ± 58	202 ± 24			
<i>Females</i>	226 ± 19	177 ± 26	404 ± 40	171 ± 14			
Liver (g)	1.10 ± 0.05	0.76 ± 0.08 *	1.11 ± 0.05	0.84 ± 0.06	P=0.036	P<0.001	P=0.367
<i>Males</i>	1.19 ± 0.07	0.84 ± 0.11	1.12 ± 0.08	0.87 ± 0.09			
<i>Females</i>	0.96 ± 0.05	0.65 ± 0.10	1.09 ± 0.06	0.78 ± 0.04			
Heart (mg)	134 ± 5	134 ± 4	136 ± 7	133 ± 8	P=0.175	P=0.874	P=0.904
<i>Males</i>	135 ± 6	139 ± 7	142 ± 10	136 ± 10			
<i>Females</i>	132 ± 8	128 ± 4	126 ± 9	126 ± 12			
Average Kidney (mg)	146 ± 6	99 ± 6 *	144 ± 5	102 ± 8	P=0.004	P<0.001	P=0.866
<i>Males</i>	157 ± 8	97 ± 12	150 ± 8	115 ± 7			
<i>Females</i>	130 ± 7	101 ± 3	134 ± 5	80 ± 1			

Brown adipose tissue (BAT); inguinal white adipose tissue (iWAT); epididymal white adipose tissue (eWAT). * P<0.05 vs. Control+Saline, and † P<0.05 vs. sRA+Saline; No significant 2-way or 3-way interactions were discovered. All data presented as mean ± sem.

Table S3. Expression of beige or brown adipose markers within iWAT – related to Figure S2.

<i>Gene</i>	<i>sRA vs control</i>	<i>p-value</i>	<i>sRA + CGP vs sRA</i>	<i>p-value</i>
Hspb7	50.914	0.00	0.392	0.07
Acot2	3.605	0.00	0.332	0.00
Pdk4	2.099	0.35	0.460	0.26
Oplah	1.729	0.03	0.753	0.31
Fbxo31	1.474	0.15	0.737	0.74
Ebf3	1.125	0.84	0.768	0.47
Slc29a1	0.871	0.49	0.796	0.64
Slc27a1	1.945	0.05	0.901	0.65
Tbx1	1.602	0.21	0.540	0.04
Klhl13	0.818	0.52	1.057	0.88
Sp100	0.473	0.02	1.591	0.33
Ear2	0.361	0.01	1.778	0.05
Tmem26	0.339	0.01	1.932	0.15
Cd40	0.310	0.01	1.945	0.36

Table S4. Expression of white adipose markers within iWAT – related to Figure S2.

<i>Gene</i>	<i>sRA vs control</i>	<i>p-value</i>	<i>sRA + CGP vs sRA</i>	<i>p-value</i>
Dpt	0.32	0.0009	2.53	0.007
Igfbp3	0.77	0.53	0.81	0.33
Hoxc8	0.77	0.46	1.45	0.16
Hoxc9	0.90	0.86	0.97	0.94
Slc7a10	0.99	0.65	1.24	0.61
Sphk1	1.11	0.85	0.95	1.00
Hoxa7	1.27	0.39	0.78	0.47

Table S5. Expression of okadaic acid-sensitive phosphatases within iWAT – related to Figure S4.

<i>Gene</i>	<i>sRA vs control</i>	<i>p-value</i>	<i>sRA + CGP vs sRA</i>	<i>p-value</i>
Ppp4c	0.70	0.14	1.17	0.62
Ppp5c	0.94	0.85	0.94	0.59
Ppp2r4	0.97	0.92	1.01	0.92
Ppp6c	0.97	0.92	1.00	0.91
Ppa1	1.45	0.07	0.93	0.61

Table S6. Expression of Creb target genes within iWAT – related to Figure 4.

<i>Gene</i>	<i>sRA vs control</i>	<i>p-value</i>	<i>sRA + CGP vs sRA</i>	<i>p-value</i>	<i>Gene</i>	<i>sRA vs control</i>	<i>p-value</i>	<i>sRA + CGP vs sRA</i>	<i>p-value</i>
Ucp1	51.625	0.00	0.030	0.00	Aass	0.829	0.66	0.908	0.81
Tac1	3.138	0.43	0.213	0.24	Syt4	0.824	0.93	0.547	0.16
Fos	2.928	0.16	2.751	0.17	Rfc1	0.807	0.35	1.064	0.80
Ndufa10	2.189	0.01	0.486	0.02	Epha2	0.801	0.37	0.933	0.96
Hk2	2.099	0.00	0.824	0.49	Dnajc3	0.796	0.27	1.206	0.33
Rgs2	1.932	0.13	0.415	0.06	Cbx4	0.796	0.27	1.275	0.29
Got1	1.778	0.03	0.570	0.02	Lmo4	0.796	0.46	1.613	0.07
Pim1	1.765	0.14	0.536	0.10	Cdc42	0.790	0.26	1.206	0.43
Homer1	1.729	0.03	0.763	0.21	Spry2	0.790	0.36	1.329	0.15
Jun	1.717	0.41	2.056	0.26	Trp53inp1	0.768	0.27	1.117	0.90
Insig1	1.647	0.11	1.125	0.42	Hoxa5	0.768	0.37	1.602	0.08
Crem	1.569	0.38	1.064	0.88	Gla	0.758	0.29	1.035	0.92
AA986860	1.558	0.41	0.763	0.99	Emd	0.753	0.38	1.133	0.77
Tob1	1.474	0.23	1.206	0.29	Asxl2	0.742	0.22	1.266	0.53
Hoxa9	1.454	0.27	0.959	0.79	Cobll1	0.737	0.24	1.602	0.06
Ube2b	1.395	0.12	0.835	0.36	Hps4	0.727	0.30	1.035	0.96
Maff	1.329	0.79	1.366	0.49	Ccn1	0.722	0.13	1.548	0.12
Psmc12	1.301	0.26	0.841	0.46	Slc2a1	0.722	0.21	0.986	0.89
Cebpb	1.292	0.52	0.812	0.40	Zfp3611	0.717	0.16	1.157	0.79
Gas1	1.275	0.52	0.637	0.23	Id2	0.717	0.19	1.162	0.86
Edf1	1.231	0.40	0.796	0.38	Son	0.712	0.19	1.283	0.47
Cpeb2	1.214	0.38	1.117	0.69	Ddx10	0.697	0.14	1.248	0.45
Nr4a2	1.173	0.78	1.064	0.71	Klf4	0.688	0.13	1.558	0.13
Idi1	1.157	0.76	1.050	0.72	Bmf	0.688	0.18	0.979	0.79
Atf3	1.141	0.85	4.857	0.01	Areg	0.683	0.42	0.191	0.21
Usp14	1.094	0.78	0.871	0.61	Piga	0.678	0.16	1.320	0.43
Ptp4a1	1.087	0.80	1.248	0.22	Rod1	0.674	0.10	1.231	0.54
Bag3	1.072	0.65	1.021	0.97	Jund	0.660	0.15	1.659	0.16
Cited2	1.028	0.62	1.050	0.96	Midn	0.655	0.08	1.198	0.58
Ube2d3	1.028	0.83	1.094	0.79	Nefl	0.624	0.68	0.160	0.86
Cyr61	1.021	0.78	3.340	0.06	Zfp3612	0.607	0.03	1.376	0.09
Junb	1.007	0.84	2.514	0.11	Gem	0.607	0.12	1.636	0.19
Ivns1abp	1.007	0.92	1.149	0.36	Cebpd	0.595	0.15	1.602	0.30
Ubl3	1.007	0.93	1.035	0.86	Hnrph1	0.591	0.06	1.376	0.35
Kiss1	1.000	1.00	1.000	1.00	Cxcl12	0.591	0.09	0.966	0.56
Etf1	0.986	0.91	1.102	0.66	Gas5	0.586	0.04	1.591	0.20
Slc7a2	0.979	0.74	0.595	0.91	Gadd45b	0.586	0.11	1.682	0.43
Nab1	0.979	0.92	1.110	0.59	Eif2c2	0.582	0.04	1.320	0.50
Ube2v1	0.966	0.89	1.007	0.97	Lif	0.582	0.09	1.310	0.19
Ets2	0.959	0.67	0.818	0.64	Hivep2	0.578	0.05	1.404	0.50
Hes1	0.953	0.72	1.064	0.43	Fus	0.574	0.02	1.464	0.15
Dusp4	0.946	0.54	1.050	0.20	Nap111	0.551	0.03	1.591	0.15
Id1	0.946	0.58	1.102	0.39	Il6	0.547	0.44	24.084	0.00
Eif1a	0.933	0.56	1.329	0.15	Btg2	0.540	0.14	3.555	0.01
Usp8	0.933	0.63	1.028	0.82	Etv5	0.529	0.07	0.966	0.56

Pck1	0.933	0.66	1.283	0.36	Slc38a2	0.497	0.02	1.454	0.20
Snrk	0.927	0.77	1.214	0.40	Nfkb2	0.497	0.02	1.329	0.70
Rnf8	0.914	0.73	0.966	0.83	Foxa2	0.486	0.75	0.651	0.80
Nr4a1	0.908	0.82	1.636	0.59	Plagl1	0.483	0.06	1.526	0.19
Adamts1	0.901	0.89	2.990	0.05	Rrad	0.480	0.11	2.056	0.19
Adam9	0.889	0.64	1.079	0.79	Bcl2	0.448	0.02	2.042	0.11
Pfkfb3	0.883	0.57	1.087	0.66	Slc20a1	0.444	0.01	2.071	0.04
Ndel1	0.883	0.59	0.966	0.96	Rgs1	0.444	0.10	2.479	0.22
Dusp1	0.865	0.71	2.621	0.11	Prrx1	0.435	0.00	1.357	0.19
Hspa5	0.835	0.40	1.257	0.41	Ddx3x	0.342	0.51	3.706	0.54
Prkar1a	0.829	0.36	1.125	0.59	Nr4a3	0.328	0.04	3.011	0.02
Hmgb2	0.829	0.62	0.973	0.57	Pesk1	0.051	0.18	33.359	0.06

Table S7. Effect of AT₂ activation and EGF on body composition – related to Figure 6.

<i>Parameter</i>	<i>Saline</i>	<i>EGF</i>	<i>CGP</i>	<i>EGF + CGP</i>	<i>EGF Main Effect</i>	<i>CGP Main Effect</i>	<i>EGF X CGP</i>
Number of mice (male)	22	22	9	19			
Age (weeks)	15	15	15	15			
Body mass (g)	26.45 ± 0.56	26.52 ± 0.53	25.21 ± 0.82	26.49 ± 0.37	P=0.113	P=0.537	P=0.463
Change in fat (g)	0.13 ± 0.17	-0.35 ± 0.13 *	0.34 ± 0.12	-0.47 ± 0.19 †	P=0.002	P=0.812	P=0.398
Change in lean (g)	0.73 ± 0.36	1.62 ± 0.44	1.16 ± 0.34	1.60 ± 0.41	P=0.169	P=0.671	P=0.641
Change in fluid (g)	0.42 ± 0.09	0.39 ± 0.11	0.64 ± 0.21	0.30 ± 0.08	P=0.138	P=0.605	P=0.204

* P<0.05 vs. Saline, and † P<0.05 vs. CGP-42122a. All data presented as mean ± sem.

Table S8. Effect of EGF on tissue masses in control and AT₂-KO mice – related to Figure 6.

<i>Parameter</i>	<i>Control Untreated</i>	<i>Control EGF</i>	<i>AT₂-KO Untreated</i>	<i>AT₂-KO EGF</i>	<i>Treatment Main Effect</i>	<i>Genotype Main Effect</i>	<i>Treatment X Genotype</i>
Number of mice (male)	6	5	7	6			
Age (weeks)	11-12	11-12	11-12	11-12			
Body mass (g)	26.84 ± 0.43	25.33 ± 0.62	27.73 ± 0.0.29	25.54 ± 0.76 *	P=0.003	P=0.315	P=0.533
iWAT (mg)	163.9 ± 12.8	117.3 ± 12.8 *	156.7 ± 11.1	142.7 ± 14.7	P=0.029	P=0.492	P=0.222
eWAT (mg)	319.5 ± 29.5	228.76 ± 8.9 *	313.2 ± 18.8	238.4 ± 24.9 *	P=0.002	P=0.943	P=0.729
BAT (mg)	58.45 ± 4.5	54.5 ± 7.8	59.1 ± 4.3	62.1 ± 10.8	P=0.951	P=0.570	P=0.636

Epidermal growth factor (EGF); inguinal white adipose tissue (iWAT); epididymal white adipose tissue (eWAT); brown adipose tissue (BAT). * P<0.05 vs. Untreated. All data presented as mean ± sem.

Table S9. Genes exhibiting significant changes in expression within iWAT that implicate electron carrier activity when analyzed by GSEA (sRA 2.00, FDR 0.0001 vs. sRA + CGP -2.04, FDR 0.0000) – related to Figure 7.

<i>Gene</i>	<i>Full name</i>	<i>sRA vs control</i>	<i>p-value</i>	<i>sRA + CGP vs sRA</i>	<i>p-value</i>
Gpx2	Glutathione peroxidase 2	10.778	0.0125	0.005	0.0001
Txndc2	Thioredoxin domain-containing protein 2	9.580	0.5433	0.087	0.4041
Asph	Aspartate beta-hydroxylase	5.352	0.0003	0.337	0.0059
Rdh16	Retinol dehydrogenase 16	4.993	0.0382	0.346	0.0571
Cycc	Cytochrome c	2.751	0.0028	0.646	0.2135
Etfdh	Electron-transferring-flavoprotein dehydrogenase	2.751	0.0011	0.473	0.0218
Me1	NADP-dependent malic enzyme	2.395	0.0309	0.763	0.8596
Idh3b	Isocitrate dehydrogenase 3 (NAD+) beta	2.362	0.0101	0.473	0.0284
Dld	Dihydrolipoamide dehydrogenase	2.189	0.0075	0.595	0.0873
Cyc1	Cytochrome c1	2.173	0.0116	0.486	0.0157
Ndufs2	NADH dehydrogenase Ubiquinone Fe-S Protein 2	2.173	0.0045	0.497	0.0090
Ndufs1	NADH dehydrogenase oxidoreductase core subunit S1	2.071	0.0113	0.566	0.0385
Cox5a	Cytochrome C oxidase subunit Va	2.056	0.0182	0.540	0.0334
Ndufs8	NADH dehydrogenase Ubiquinone Fe-S Protein 8	2.014	0.0119	0.463	0.0045
Aldh4a1	Aldehyde dehydrogenase 4 family member A1	1.972	0.0077	0.674	0.2907
Etfb	Electron-transfer-flavoprotein, Alpha polypeptide	1.972	0.0136	0.660	0.1561
Ndufa9	NADH dehydrogenase Ubiquinone 1 alpha subcomplex 9	1.959	0.0193	0.555	0.0382
Etfb	Electron-transfer-flavoprotein, Beta polypeptide	1.919	0.0498	0.651	0.2090
Sdhb	Succinate dehydrogenase complex, subunit D, integral membrane protein	1.905	0.0242	0.620	0.1085
Ndufs3	NADH dehydrogenase Ubiquinone Fe-S Protein 3	1.866	0.0174	0.599	0.0449
Ndufs4	NADH dehydrogenase Ubiquinone Fe-S Protein 4	1.866	0.0214	0.688	0.1553
Aifm1	Apoptosis-inducing factor, mitochondrion-associated, 1	1.853	0.0226	0.603	0.0825
Uqcrl1	Ubiquinol-cytochrome C reductase, complex II Subunit XI	1.853	0.0360	0.563	0.0574
TXNRD2	Thioredoxin reductase 2	1.778	0.0566	0.607	0.0753
Phyh	Phytanoyl-CoA 2-hydroxylase	1.717	0.0690	0.732	0.4656
Ndufs7	NADH dehydrogenase Ubiquinone Fe-S protein 7	1.682	0.0461	0.655	0.1131
Dhhdh	Dihydrodiol dehydrogenase	1.647	0.0623	0.796	0.4064
Ndufa13	NADH dehydrogenase Ubiquinone 1 alpha subcomplex 13	1.625	0.0613	0.669	0.1376
Fxn	Fraataxin	1.485	0.2213	0.611	0.1410
Nqo1	NADH dehydrogenase, Quinone1	1.424	0.1643	0.637	0.0697
Cyb561	Cytochrome B561	1.310	0.8280	0.582	0.6477
Qdpr	Quinoid dihydropteridine reductase	1.292	0.2952	0.859	0.6280
Aldh2	Aldehyde dehydrogenase 2	1.257	0.2743	0.859	0.6857
Maob	Manoamine oxidase B	1.257	0.3944	0.979	0.7289
Cox11	Cytochrome C oxidase copper chaperone	1.248	0.4116	0.908	0.6254
Fdx1	Ferredoxin 1	1.240	0.4728	0.979	0.9750
Cyb5r3	Cytochrome B5 reductase 3	1.206	0.5940	0.774	0.4083
Adh5	Alcohol dehydrogenase 5 (Class III), Chi polypeptide	1.173	0.5065	0.959	0.9613

Sardh	Sarcosine dehydrogenase	1.125	0.6786	0.859	0.7535
Nqo2	NADH dehydrogenase, Quinone 2	1.110	0.6952	0.779	0.3019

Note: Out of 71 total genes in the electron carrier activity gene set, these are the only 40 genes identified by GSEA analysis to be part of the GSEA core enrichment set.

Supplemental Experimental Procedures

Comprehensive Laboratory Animal Monitoring System (CLAMS)

Metabolic parameters were assessed throughout the light cycle using a “comprehensive lab animal monitoring system (OxyMax/CLAMS)” (Columbus Instruments) apparatus. Ambient temperature was maintained at thermoneutrality (30°C). Following a 48-hour acclimatization period, food intake, spontaneous physical activity via photoelectric beam break, and heat production by respirometry were measured over an additional 48 hours. Data were averaged during the light cycle, dark cycle, or 24-hour recordings for each mouse.

Indirect calorimetry

To determine resting metabolic activity, we used a continuous respirometry system (AEI). Briefly, mice were placed in a warmed water-jacketed 2 L beaker (Ace Glass, Vineland, NJ) that had an air flux of 300 mL/min. Effluent air (300 mL/min, STP-corrected) was dried (CaSO₄ Drierite, Arcos) and subsampled for analyses of oxygen and carbon dioxide content (AEI S-3A/II & CD-31, respectively). Heat production was calculated using the formula derived from Lusk (Lusk, 1928).

Plasma collection

Blood was collected from the submandibular vein using a lancet (Medipoint) or from the trunk following asphyxiation and decapitation, and collected in lithium-heparin coated tubes (Sarstedt). After centrifugation of whole blood at 5,000 xg for 5 minutes, the supernatant was collected and stored at -80°C until further analysis.

Metabolic cages / Bomb calorimetry

Mice were housed in Nalgene (Rochester, NY) single-mouse sized metabolism cages over three nights with *ad libitum* access to water and powdered chow (Harlan Teklad 7013). Data from the second and third nights were averaged for each mouse. Food, urine, and fecal samples from the last 24 hours in metabolism cages were collected and the food and fecal samples were dried overnight at 55°C. Caloric densities of the food and dried feces were determined in a 50 mg semi-micro bomb calorimeter (Parr Instrument Co, Moline, IL) calibrated with benzoic acid. Caloric loss to feces was subtracted from caloric intake to calculate daily caloric absorption for each mouse, and digestive efficiency was calculated as the fraction of calories absorbed per calories consumed.

In Vivo Glucose Uptake Assay

Adult (12-20 week old) mice were fasted overnight. Tail blood was collected from all mice (time=0) followed by an injection (i.p.) of 8-10 μ Ci of [3H]-2-deoxyglucose in a 20% glucose solution. Over the course of 1 hour, tail blood was collected (15, 30, and 60 min). After 1 hour, mice were sacrificed via decapitation and tissues were isolated and flash-frozen in liquid nitrogen to measure plasma radioactivity and [3H]-2-deoxyglucose uptake in tissues. Plasma radioactivity and [3H]-2-deoxyglucose uptake in tissues was analyzed as previously described (Markan et al., 2014).

Body Composition

Body composition was determined using nuclear magnetic resonance (LF90, Bruker). Briefly, mice were placed in a restraint tube without anesthesia for the 1-2 minute procedure, then immediately returned to home cages.

Sympathetic Nerve Activity

After 8 weeks of saline or CGP-42112a treatment, control and sRA mice were initially anesthetized with an i.p. injection of ketamine/xylazine and the anesthetic plane was sustained throughout the protocol with intravenous infusion of alpha-chloralose (25 mg/kg during surgical preparation and then 6 mg/kg/hr during the experimental protocol) through the left jugular vein. Mice were intubated with PE-50 for spontaneous respiration of oxygen-enriched room air. The left carotid artery was cannulated for continuous blood pressure measurement. Body temperature was maintained at 37.5°C with the use of a colonic temperature probe. After exposing the inguinal fat pad, the sympathetic nerve innervating the adipose tissue was isolated. Using a 36-gauge platinum-iridium electrode, a nerve was suspended and secured in place with silicone gel (World Precision Instruments). The nerve signal was amplified (100,000 x) and filtered at the low and high frequency cutoff of 100 and 1000 kHz respectively using a Grass P5 AC preamplifier. The amplified and filtered nerve signal was routed to a resetting voltage integrator (model B600c, University of Iowa Bioengineering) and to a PowerLab unit and its associated Chart software (ADInstruments) which measured the same amplified and filtered nerve signal as spikes/sec that exceeded baseline noise. A stable period of 20-30 minutes was used to initially record inguinal sympathetic activity from an

intact nerve. Next, the inguinal nerve was cut distal from the recording site to measure efferent activity from the same nerve for an additional 20-30 minutes. Data were recorded and analyzed on a Macintosh computer.

3T3-L1 cell culture

3T3-L1 preadipocytes were cultured in preadipocyte media (DMEM-High Glucose without pyruvate, 10% FBS, 1% penicillin/streptomycin). When cells were 100% confluent (Day 0), media was changed to induction media (preadipocyte media with 1 mM IBMX, 1 U/mL insulin, and 1 μ M dexamethasone). After two days, media was replaced with maintenance media (preadipocyte media with insulin (1 U/mL), which was replaced every 2 days thereafter. Before treatment, cells were serum-starved overnight (DMEM-HG and 1% Pen/Strep). Cells were treated with CGP-24114a (Sigma; 0.1 nM, 10 nM), PD-123,319 (Sigma; 10 μ M), or losartan (Sigma; 10 μ M).

Primary adipocyte culture

Inguinal white adipose tissue or interscapular brown adipose tissue was collected from 4 day-old wild-type C57BL/6J, AT₂-KO, or littermate-control pups as indicated. Tissue was incubated in collagenase type 2 (Worthington) solution (1 mg/mL collagenase, 2% BSA in Hanks' Balanced Salt solution) at 37°C for 1 hr on a rocker. Stromal vascular fraction, which contained the preadipocytes, was isolated and washed with preadipocyte growth media (DMEM-HG, 10% FBS, 1% Pen/Strep, 1X non-essential amino acid, 1X glutamax, 20 mM hepes (pH 7.3), 0.1 mM β -mercaptoethanol). Cells were plated in preadipocyte growth media (1 well per pup), which was replaced every 2 days. 2 days after cells reach 100% confluency (Day 0), media was replaced with differentiation media (DMEM-HG, 10% FBS, 1% Pen/Strep, 5 μ g/mL insulin, 1 μ M dexamethasone, 0.5 mM isobutylmethylxanthine, 1 μ M rosiglitazone). On Day 2, media was replaced with adipocyte maintenance media (DMEM-HG, 10% FBS, 1% Pen/Strep, 5 μ g/mL insulin), which was replaced every 2 days thereafter. Differentiation and maintenance media was supplemented with EGF (AbD Serotec; 1 ng/mL) or EGF and CGP (10 or 100 nM) as indicated.

Immortalized human preadipocyte/adipocyte culture

Briefly, subcutaneous preadipocytes derived from a 38-year old non-diabetic female donor (Lonza lot #0000279746) were immortalized with TERT and HPV E6/E7. For the current studies, a stable diploid clone (referred to as clone B) with consistent differentiation capacity was isolated by ring cloning. Cells were grown in preadipocyte PGM2 media (Lonza). Once cells were confluent, differentiation was induced by incubation in differentiation media consisting of dexamethasone, IBMX, indomethacin, and additional insulin (Lonza) according to the manufacturer's instructions. Cells were differentiated for 10 days. Prior to treatment, media was replaced with PGM2 media for one day and then switched to serum-free media overnight for treatments. Adipocytes were treated for 6 hours with vehicle, NE (Hospira; 10 μ M), CGP (Sigma; 10 nM), or NE and CGP.

Oil Red O staining

Differentiation and maintenance media were supplemented with vehicle, EGF (1 ng/mL), and/or CGP (10 or 100 nM). On day 4 of differentiation, cells were washed with 1X PBS and then fixed with 10% formalin for at least 1 hour. After washing with 60% isopropanol, wells were allowed to dry completely. Oil Red O was added for 10 min and then washed four times with water. To assess red-stained area fraction, color channels were split, and identical intensity thresholds were set for all images before area fraction analyses.

Chromatin immunoprecipitation (ChIP)

ChIP was performed essentially as previously described (Weatherford et al., 2012). Antibodies against CREB (catalog #9197) and IgG (#2729) were purchased from Cell Signaling Technology (Danvers, MA). Primers for UCP1 were: 5'-AAGCTTGCTGCTCACTCCTCT-3' and 5'-TAATGGAGAGAGCAGTAGGG-3'.

Cellular respiration

Differentiation and maintenance media were supplemented with vehicle, EGF (1 ng/mL), and/or CGP (10 nM). On day 4 of differentiation, the media was exchanged with a XF prep station (Seahorse Biosciences) to XF assay medium (Seahorse Biosciences) supplemented with 25 mM glucose, 1 mM pyruvate, and 2 mM L-glutamine. The assay medium was adjusted to pH 7.4 (37°C) before to use with the media buffer capacity determined before each experiment using established Seahorse Biosciences protocols. Cells were then incubated for 30 min at 37°C in a non-CO₂ incubator and their metabolic profiles were subsequently assayed using the XF-96 Extracellular Flux Analyzer (Seahorse Biosciences) following manufacturer recommended protocols.

Cyclic Nucleotide and Peptide Assays

cGMP, cAMP, and ANP levels were analyzed using a cyclic GMP EIA kit (Biomedical Technologies Inc.), cyclic cAMP EIA kit (Cayman Chemical), and ANP EIA kit (Phoenix Pharmaceuticals, Inc.) respectively according to the manufacturers' instructions.

Gene expression

Total RNA from tissues or cells was extracted in Trizol (Life Technologies) and isolated using RNA Purelink Minikit (Invitrogen) as per the manufacturer protocol. RNA underwent RT-PCR using SuperScript III (Invitrogen) followed by real-time PCR. Human UCP1 expression was determined using TaqMan (Applied Biosystems). All other gene expressions were determined using SYBR-green assays and primer sets from Applied Biosystems. Gene expression levels were compared using the Livak method (Livak and Schmittgen, 2001).

The following primers were used:

<i>18S rRNA</i>	forward (f) 5'-aggggagagcgggtaagaga-3'	reverse (r) 5'-ggacaggactaggcgggaaca-3'
<i>β-actin</i>	(f) 5'-catcctcttctccctggagaaga-3'	(r) 5'-acaggattccataaccaagaaggaagg-3'
<i>Cidea</i>	(f) 5'-tgctcttctgtatcggccagt-3'	(r) 5'-gccgtgtaaggaatctgctg-3'
<i>Colipase</i>	(f) 5'-acacacaaggccatggagaa-3'	(r) 5'-tcacagggacaccggtagt-3'
<i>Eval</i>	(f) 5'-cacttctctgagtttacagc-3'	(r) 5'-gcattttaaccgaacatctgtcc-3'
<i>Lipase</i>	(f) 5'-gccaggatgccagaagaata-3'	(r) 5'-acaggcagcaaagtctcgag-3'
<i>NPR-A</i>	(f) 5'-cgaagacaagtgcacctcag-3'	(r) 5'-tggagacacagtcaacacagc-3'
<i>NPR-C</i>	(f) 5'-agctggcatcagcaagaagg-3'	(r) 5'-cggcgataccttcaaatgc-3'
<i>PGC-1α</i>	(f) 5'-agccgtgaccactgacaacgag-3'	(r) 5'-gctgcatgggtctgagtgctaag-3'
<i>Renin</i>	(f) 5'-tgaagaaggctgtgcggtagt-3'	(r) 5'-tcccagggtcaaaggaaatgc-3'
<i>UCP1</i>	(f) 5'-gtgaaggtcagaatgcaagc-3'	(r) 5'-agggcccccctcatgaggtc-3'
<i>UCP2</i>	(f) 5'-acaagaccattgcacgagag-3'	(r) 5'-catggttaaggcagtgac-3'
<i>UCP3</i>	(f) 5'-atgcatgcctacagaacat-3'	(r) 5'-ctggccaccatcctcagca-3'

Immunoblot analysis

Following 5 min treatment with vehicle, NE (1 μM), or NE and CGP (10 nM), cells were lysed using a RIPA buffer (1% Nonidet P-40, 0.5% deoxycholate, and 0.1% SDS in 1X PBS with 1X proteinase inhibitor and 1X phosphatase inhibitor mixture). Cell lysates were centrifuged, and protein was quantified using the Pierce BCA Protein Assay Kit (Thermo scientific). 20 μg of protein were run on a 10% SDS-PAGE and transferred to an Immun-Blot Polyvinylidene Difluoride Membrane (Bio-Rad). Membranes were blocked with 5% BSA and immunoblotted with primary antibody: Anti-phospho-Creb at ser133 (Cell Signaling; catalog no. 87G3), anti-Creb (Cell Signaling; catalog no. 9197S), anti-beta actin (Abcam; catalog no. ab8227) followed by ECL anti-rabbit IgG, HRP conjugate antibody (Amersham Bioscience). Bands were detected with ECL (Amersham Biosciences) and quantified using ImageJ software.

Supplemental References

Livak, K.J., and Schmittgen, T.D. (2001). Analysis of relative gene expression data using real-time quantitative PCR and the 2(-Delta Delta C(T)) Method. *Methods* 25, 402-408.

Lusk, G. (1928). *The elements of the science of nutrition*. (Philadelphia, PA: W.B. Saunders Company).

Markan, K.R., Naber, M.C., Ameka, M.K., Anderegg, M.D., Mangelsdorf, D.J., Kliewer, S.A., Mohammadi, M., and Potthoff, M.J. (2014). Circulating FGF21 is liver derived and enhances glucose uptake during refeeding and overfeeding. *Diabetes* 63, 4057-4063.

Weatherford, E.T., Liu, X., and Sigmund, C.D. (2012). Regulation of renin expression by the orphan nuclear receptors Nr2f2 and Nr2f6. *American journal of physiology. Renal physiology* 302, F1025-1033.